Journal of Cardiology 73 (2019) 163–170

Contents lists available at ScienceDirect

Journal of Cardiology

journal homepage: www.elsevier.com/locate/jjcc

Original article

Global strain and dyssynchrony of the single ventricle predict adverse cardiac events after the Fontan procedure: Analysis using feature-tracking cine magnetic resonance imaging

Umiko Ishizaki (MD)[a], Michinobu Nagao (MD PhD)[a,*], Yumi Shiina (MD PhD FJCC)[b,c], Kei Inai (MD PhD FJCC)[b,d], Hiroki Mori (MD)[d], Tatsunori Takahashi (MD)[d], Shuji Sakai (MD PhD)[a]

[a] Department of Diagnostic imaging & Nuclear Medicine, Tokyo Women's Medical University, Tokyo, Japan
[b] Department of Pediatric Cardiology, Division of Clinical Research for ACHD, Tokyo Women's Medical, Tokyo, Japan
[c] Cardiovascular Center, St. Luke's International Hospital, Tokyo, Japan
[d] Department of Pediatric Cardiology, Tokyo Women's Medical University, Tokyo, Japan

ARTICLE INFO

Article history:
Received 25 March 2018
Received in revised form 14 June 2018
Accepted 17 July 2018
Available online 3 September 2018

Keywords:
Fontan procedure
Prognosis
Cardiac magnetic resonance imaging
Myocardial strain
Feature tracking

ABSTRACT

Background: The aim of this study was to determine whether major adverse cardiac events (MACE) during the late phase of the Fontan procedure could be predicted by strain measurements of single ventricles using cardiac magnetic resonance imaging with feature tracking (CMR-FT).
Methods: One hundred adolescent patients who underwent the Fontan procedure (mean age, 21 years) were examined retrospectively with CMR-FT to assess the systemic single-ventricle function. Vertical long-axis cine imaging was divided into six myocardial segments. Global longitudinal strain (GLS) was determined by averaging the peak strain values of each of the six segments. The dyssynchrony index was defined as the standard deviation of the time to peak strain for six segments. The primary outcome was MACE, defined as cardiac death and unscheduled hospitalization.
Results: MACE occurred in 18 patients during a mean follow-up of 62 months. According to the multivariate logistic regression analysis results for potential predictor variables, GLS and the dyssynchrony index are independent predictors of MACE. Patients with GLS $\geq$11.8% had significantly higher MACE-free rates than did those with GLS $<$11.8% [log-rank value, 14.15; $p = 0.0002$; hazard ratio, 6.82; 95% confidence interval (CI), 2.51–18.56]. Patients with a dyssynchrony index $<$63.5 ms had significantly higher MACE-free rates than did those with dyssynchrony index $\geq$63.5 ms (log-rank value, 28.17; $p < 0.0001$; hazard ratio, 21.69; 95% CI, 6.96–67.56).
Conclusion: GLS and the dyssynchrony index found using CMR-FT are independent predictors of MACE for adolescent patients after the Fontan procedure and provide information regarding risk stratification beyond clinical parameters and biomarkers.

Introduction

Although postoperative mortality rates in patients after the Fontan procedure have dramatically improved [1–3], the long-term mortality rates have remained high compared to those in patients with other types of congenital heart disease (CHD) [4]. Patients may be affected by ventricular dysfunction after Fontan palliation, and heart failure symptoms have been reported in up to 40% during long-term follow-up [5–7]. Therefore, a reliable analysis of systolic ventricular function is of interest; however, it is hampered by complexities. In addition, as for other patients with CHD, established volumetric measurements of systolic function, such as ejection fraction (EF), may lack sensitivity in detecting early myocardial dysfunction [8–10].

Unfortunately, reliable assessments of ventricular deformation using echocardiography involve complex ventricular anatomy and physiology associated with CHD [11,12]. In

* Corresponding author at: Department of Diagnostic Imaging and Nuclear Medicine, Tokyo Women's Medical University, 8-1 Kawada-cho, Shinjuku-ku, Tokyo 162-8666, Japan.
E-mail address: nagao.michinobu@twmu.ac.jp (M. Nagao).

https://doi.org/10.1016/j.jjcc.2018.07.005
0914-5087/

addition, the evaluation of CHD patients is frequently limited by poor acoustic windows [13]. Cardiac magnetic resonance with feature tracking (CMR-FT) has emerged as a useful tool for quantitative wall motion analysis and allows quantification of biventricular mechanics using measurements of deformation such as strain and dyssynchrony [14,15]. Therefore, the utilities of CMR-FT in detecting early myocardial damage compared to volumetric methods should be mentioned more. Nonetheless, the global strain and dyssynchronous contraction of functional single ventricles in Fontan patients have not been explored [16]. The purpose of this study was to determine whether adverse cardiac events during the late phase of the Fontan procedure could be predicted by myocardial strain measurements of the single ventricle using CMR-FT.

Methods

Patient population

This retrospective cohort study was approved by the institutional research ethics board and included 100 consecutive adolescent patients and adult patients who underwent the Fontan procedure between April 2002 and December 2016. All patients underwent CMR, cardiac catheterization, transthoracic echocardiography, 12-lead electrocardiogram (ECG), and clinical examination at the same time as part of their routine follow-up, and their clinical/surgical history and New York Heart Association (NYHA) functional class were collected from medical records. During the same time period, seven patients were contraindicated to CMR due to implant of pacemaker or cardiac resynchronization therapy (CRT). These patients were excluded from this study. Furthermore, a group of patients with optimal clinical status characterized by NYHA functional class I or II, brain natriuretic peptide (BNP) levels <300 pg/mL, maximum exercise work load ≥ 100 W, and no history of significant clinical events such as arrhythmias or heart failure was defined as the reference cohort. Central venous pressure, pulmonary artery wedge pressure, and single ventricle end-diastolic pressure as hemodynamic measurements were obtained from cardiac catheterization within three months of CMR. Heterotaxy syndrome was identified based on the reviews of echocardiographic, computed tomography, CMR, and postoperative findings using the criteria proposed by Van Praagh and colleagues [17]. The presence of atrioventricular valve regurgitation was diagnosed by CMR and echocardiography. Indications for the initial Fontan procedure included various types of CHD (Table 1).

Major adverse cardiac events

Major adverse cardiac events (MACE) related to Fontan pathophysiology and defined as those requiring unscheduled hospitalization included arrhythmias, heart failure, hemostatic complications (including thromboembolism and hemoptysis), catheterization and/or surgical intervention, and death. Patients were categorized as having heart failure if there was evidence of at least one of the following: orthopnea, nocturnal dyspnea, pulmonary edema, increasing peripheral edema, or radiological signs. Protein-losing enteropathy (PLE), its relapse, and renal

Table 1
Patients characteristics.

Characteristics	Total ($n=100$)	MACE ($n=18$, 18%)	Non-MACE ($n=82$, 82%)	p value
Female	52 (52%)	9 (50%)	43 (52%)	0.851
Diagnosis				
SRV/SLV	37 (37%)	6 (33%)	31 (38%)	
DORV/TGA	33 (33%)	9 (50%)	24 (29%)	
TA	21 (21%)	2 (11%)	19 (23%)	
PAIVS	7 (7%)	0 (0%)	7 (8.5%)	
AVSD	2 (2%)	1 (5.6%)	1 (1.2%)	
AVVR	16 (16%)	5 (27%)	11 (13%)	0.156
Heterotaxy	23 (23%)	6 (33%)	17 (21%)	0.266
APC-Fontan ope.	68 (68%)	15 (83%)	53 (65%)	0.166
Age at Fontan ope. (years)	6.5 ± 6.5	10.1 ± 8.3	5.8 ± 5.8	0.017
Time between Fontan ope. and cardiac MRI (years)	15.0 ± 5.7	17.6 ± 6.0	14.4 ± 5.4	0.033
Physical examination				
Heart rates (beats/min)	71.4 ± 11.7	74.6 ± 8.0	70.1 ± 12.3	0.221
SpO_2 (%)	93.1 ± 3.6	92.2 ± 3.7	93.3 ± 3.5	0.239
6MWT (m)	500.2 ± 62.9	471.1 ± 57.3	507.5 ± 62.6	0.062
NYHA I/II	66/34	7/11	59/23	0.012
Laboratory examination				
BNP (pg/mL)	78.9 ± 63.7	96.1 ± 78.1	75.0 ± 59.8	0.710
ECG				
QRS width (ms)	105 ± 18	102 ± 15	106 ± 19	0.455
Catheterization				
CVP (mmHg)	12.5 ± 2.7	12.9 ± 2.4	12.4 ± 2.7	0.438
PA wedge (mmHg)	7.8 ± 2.5	8.2 ± 2.9	7.6 ± 2.3	0.425
SV-EDP (mmHg)	7.9 ± 3.2	8.9 ± 4.3	7.5 ± 2.6	0.107
Cardiac MRI				
SV-EDVI (mL/m^2)	91.7 ± 30.7	102.1 ± 33.5	88.7 ± 29.4	0.102
SV-EF (%)	48.3 ± 10.5	47.0 ± 12.3	48.6 ± 10.1	0.027
Global longitudinal strain (%)	14.0 ± 4.7	10.6 ± 4.8	14.7 ± 4.4	0.0004
Dyssynchrony index (ms)	50.2 ± 27.0	69.0 ± 27.2	46.1 ± 25.2	0.005

SRV, single right ventricle; SLV, single left ventricle; DORV, double outlet right ventricle; TGA, transposition of the great arteries; TA, tricuspid atresia; PAIVS, pulmonary atresia with intact ventricular septum; AVSD, atrio-ventricular septal defect; AVVR, atrioventricular valve regurgitation; APC, atrio-pulmonary connection; 6MWT, six-minute walk test; NYHA, New York Heart Association; BNP, brain natriuretic peptide; CVP, central venous pressure; PA, pulmonary artery; SV-EDP, single ventricle-end diastolic pressure; SV-EDVI, single ventricle-end diastolic volume index; SV-EF, single ventricle-ejection fraction.

failure were categorized as heart failure. Deaths were defined as sudden when they occurred within 1 h of acute symptoms, and they were classified as secondary to heart failure when they occurred after progressive worsening heart failure. Follow-up data were obtained from hospital records. In cases of multiple events, the censoring event was the first sequential event. Decisions regarding total cavo-pulmonary connection (TCPC) conversion for hemodynamic abnormalities in atrio-pulmonary connection (APC) Fontan patients and coil embolization for venous collaterals were made at our clinical conferences. Therefore, scheduled TCPC conversion and catheterization were not considered cardiac events. Elective day case admissions for diagnostic investigations and ablation for atrial fibrillation were excluded from the analysis.

CMR acquisition

All CMR examinations were performed using a 1.5-T magnetic resonance imaging (MRI) scanner (GyroscanIntera and Intera; Philips Medical Systems, Best, the Netherlands) with a four-element phased-array coil in the supine position with breath-holds during expiration and ECG gating. A horizontal long-axis image and a short-axis single ventricular image stack from the atrioventricular ring to the single ventricular apex were acquired using cine-balanced turbo field-echo sequences (repetition time, 2.8 m; echo time, 1.4 ms; flip angle, 45°; slice thickness, 8 mm; field of view, 380 mm; matrix size, 176 × 193; SENSE factor 2). There were 20 phases per cardiac cycle, resulting in a mean temporal resolution of 45 ms. Single ventricular end-diastolic volume (SV-EDV) and single ventricular end-systolic volume (SV-ESV), which are the sum of the largest and smallest bi-ventricular volumes (mL), were quantified using manual planimetry of the endocardial and epicardial borders from the horizontal long-axis image stack using available software (Vitrea; Canon Medical Systems Co., Tochigi, Japan).

CMR-FT analysis

CMR-FT was undertaken using the dedicated software (Vitrea). Vertical long-axis cine imaging with cine-balanced turbo field-echo sequences passing through the center of the atrio-ventricular valve and the apex of the systematic single ventricle was used for strain measurements of the single ventricle. The atrio-ventricular valve was defined as the mitral valve for patients with transposition of great arteries and the tricuspid valve for patients with double outlet right ventricle. Endocardial and epicardial borders were manually drawn in the end-diastolic frame. Papillary muscles were excluded from the endocardial contour. These were then automatically propagated through the cardiac cycle by matching individual patterns that represent anatomical structures. These were identified by the method of maximum likelihood between the regions of interest of consecutive frames [18]. The distance moved by individual points within the two-dimensional (2D) matrix between frames permitted computation of the displacement and strain. In the case of faulty propagation, the track line can be re-adapted to the endocardial border. Then, the software propagates a new track line based on the manually made corrections.

Vertical long-axis cine imaging was divided into six myocardial segments. Endocardial global longitudinal strain (GLS) was determined by averaging the peak strain values of each of the six segments. The dyssynchrony index (ms) was defined as a standard deviation of the time to peak strain for six segments while considering the differences in the timing of strain changes for all myocardial segments during systole [19,20] (Fig. 1).

Statistical analysis

Data are expressed as mean ± standard deviation (SD) for normally distributed continuous variables, median (range) for skewed continuous variables, and counts (percentage of total) for categorical variables. The absolute values of global GLS were used to facilitate interpretation and analyses. Testing of differences in demographic and clinical data based on MACE and non-MACE was accomplished with either the unpaired Student t test or the Wilcoxon rank sum test for continuous variables, and with either Pearson's chi-square test or Fisher's exact test for categorical variables, as appropriate. Comparisons of CMR measurements among the three types of dominant ventricles were analyzed using the Tukey–Kramer method and one-way ANOVA. Measures of the association between potential predictor variables and MACE were first determined by univariate logistic regression. Covariates with $p < 0.05$ during univariate testing were considered for inclusion in a multivariate model to identify factors independently associated with MACE. Covariates were retained during the final multivariate model if $p < 0.05$ or if they showed evidence of significant confounding or effect modification. A receiver-operating characteristic (ROC) curve analysis was performed to determine the optimal cut-off for the GLS and dyssynchrony index for the prediction of MACE. Survival curves of the patient subgroups were created using the Kaplan–Meier method to clarify the time-dependent cumulative MACE-free rates and were compared using the log-rank test. A Cox proportional hazards regression analysis was performed to evaluate the factors that were associated with the development of MACE. Statistical significance was established using a two-tailed p-value <0.05. All statistical analyses were performed using the JMP statistical program package (version 9.0; JMP, Inc., Cary, NC, USA).

Results

The mean follow-up period after cardiac MRI was 62.3 months (median, 63 months; range, 3–131 months). Of the cohort of 100 patients, 38% had a systemic left ventricle, 68% had an atrio-pulmonary (AP) Fontan procedure (revised AP Fontan was considered an extracardiac or lateral tunnel accordingly), mean age at cardiac MRI was 21.4 years (median, 21.5 years; range, 6–45 years), and mean time from the Fontan procedure to cardiac MRI was 15.0 years (median, 18.5 years; range, 5–32 years). MACE occurred in 18 patients (outcomes: death, 3; unscheduled hospitalization, 15). Of the 15 patients with unscheduled hospitalizations, 10 patients with heart failure, 3 patients with PLE, 3 patients with sustained ventricular tachycardia, and 1 patient who underwent intra-ventricle thrombectomy were observed. CRT was performed for the four patients with refractory heart failure.

Clinical features of Fontan patients with or without MACE are summarized in Table 1. Compared with the Fontan patients without MACE, those with MACE were statistically significantly older at the time of the Fontan procedure and had prolonged time between the Fontan procedure and cardiac MRI. Regarding the dominant ventricle type, the 18 patients with MACE included 4 with a left ventricle, 4 with a right ventricle, and 10 with bi-ventricles. There was no significant difference in the GLS, dyssynchrony index, and single ventricular ejection fraction (SV-EF) among the three types. The SV-EDV index was significantly greater for patients with bi-ventricle types than for those in other groups (Table 2).

Potential risk factors for MACE were identified by univariate logistic regression (Table 3). Although the time between the Fontan procedure and cardiac MRI, SV-EDV index, SV-EF, GLS, and dyssynchrony index were identifiable risk factors for MACE during

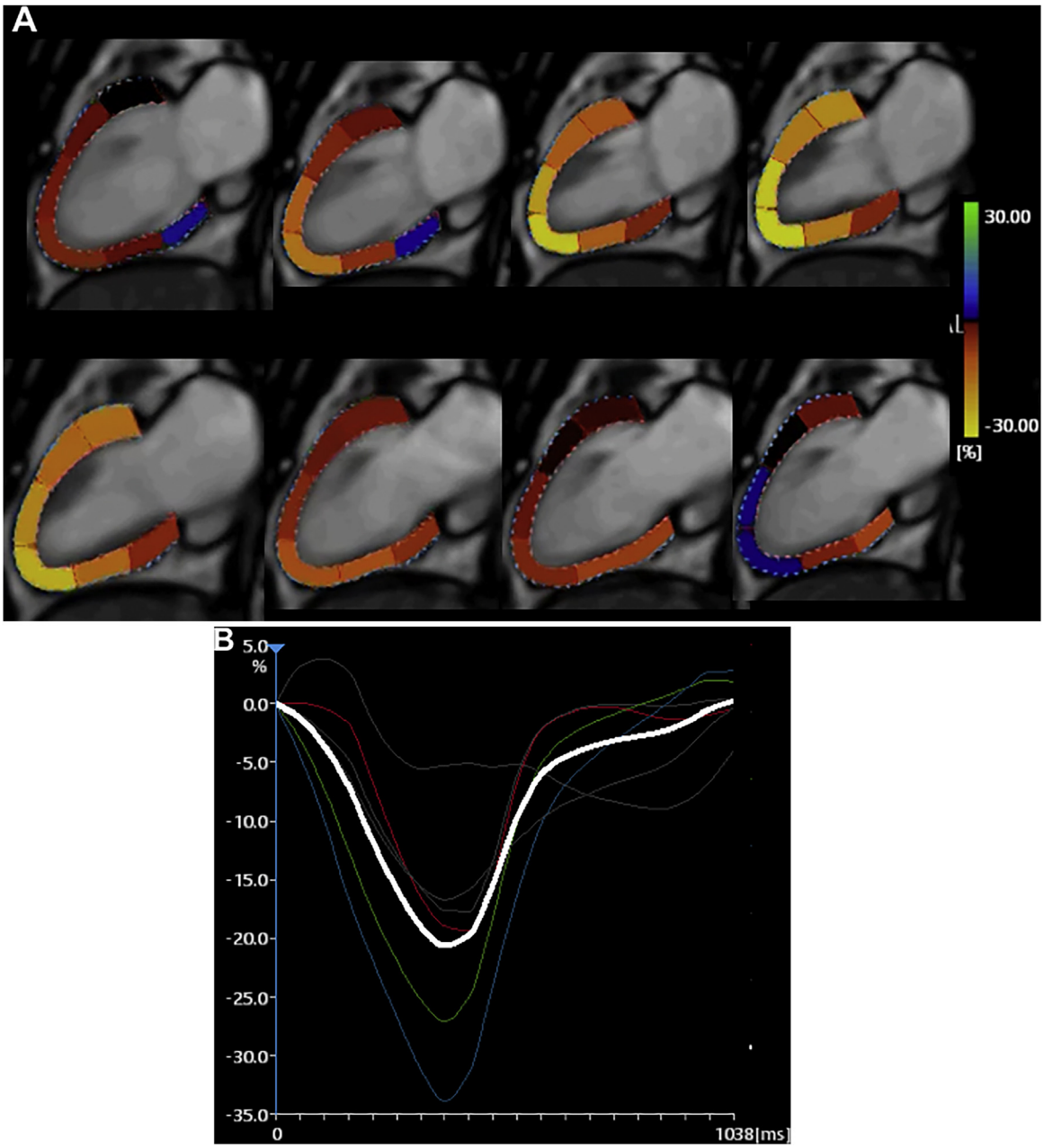

Fig. 1. A woman in her 20s without major adverse cardiovascular events who underwent the atrio-pulmonary connection Fontan operation for tricuspid atresia, aortic coarctation, patent ductus arteriosus, and atrial septal defect 13 years previously. (A) Feature-tracking analysis of vertical long-axis cine imaging shows color-coded strain values for six myocardial segments throughout a cardiac cycle. Upper row is systole; lower row is diastole. Hot colors represent large strain value; cold colors represent small strain values. (B) Time curves of longitudinal strain for six segments and global strain (white) show almost the same peak time of strain values. Her global longitudinal strain and dyssynchrony index were 21% and 31 ms, respectively.

Table 2
Cardiac MR measurement by the dominant ventricle types.

Variables	Left ventricle ($n=38$)	Right ventricle ($n=26$)	Bi-ventricle ($n=36$)	p value
SV-EDVI (mL/m^2)	82.4 ± 32.3	82.5 ± 29.1	105.9 ± 25.3	0.003
SV-EF (%)	49.2 ± 10.1	46.3 ± 12.7	49.0 ± 8.8	0.603
Global longitudinal strain (%)	14.3 ± 4.5	13.1 ± 5.4	14.2 ± 4.4	0.652
Dyssynchrony index (ms)	48.8 ± 26.3	50.3 ± 28.4	52.5 ± 29.3	0.859

SV-EDVI, single ventricle-end diastolic volume index; SV-EF, single ventricle-ejection fraction.

univariate logistic regression, the GLS and dyssynchrony index (odds ratio, 0.84 and 1.01; 95% confidence interval, 0.70–0.98 and 1.00–1.04) remained independent predictors of MACE during multivariate testing.

A ROC curve analysis revealed that the GLS and dyssynchrony index were 11.8% and 63.5 ms for predicting patients with MACE, with areas under the curve of 0.74 and 0.74, sensitivities of 72% and 72%, and specificities of 74% and 83%, respectively. Patients with

Table 3
Factors associated with MACE.

Variable	Univariate analysis OR (95%CI)	*p* value	Multivariate analysis OR (95%CI)	*p* value
Female	1.10 (0.39–3.10)	0.851		
AVVR	2.48 (0.69–8.13)	0.141		
Heterotaxy	1.91 (0.59–5.72)	0.256		
Age at Fontan ope. (years)	1.09 (1.01–1.17)	0.016	1.08 (0.99–1.18)	0.086
Time between Fontan ope. and cardiac MRI (years)	1.10 (1.00–1.22)	0.039	1.09 (0.96–1.27)	0.197
Physical examination				
Heart rates (beats/min)	1.03 (0.98–1.07)	0.218		
SpO_2 (%)	0.92 (0.80-1.06)	0.236		
Laboratory examination				
BNP (pg/mL)	1.00 (0.99–1.01)	0.216		
ECG				
QRS (ms)	0.99 (0.9–1.02)	0.464		
Catheterization				
CVP (mmHg)	1.01 (0.88–1.32)	0.434		
PA wedge (mmHg)	1.09 (0.88–1.37)	0.426		
SV-EDP (mmHg)	1.15 (0.97–1.38)	0.112		
Cardiac MRI				
SV-EDVI (mL/m^2)	1.01 (0.99–1.03)	0.107		
SV-EF (%)	0.93 (0.88–0.98)	0.014	0.97 (0.91–1.03)	0.353
Global longitudinal strain (%)	0.80 (0.68–0.91)	0.002	0.84 (0.70–0.98)	0.038
Dyssynchrony index (ms)	1.02 (1.01–1.03)	0.005	1.01 (1.00–1.04)	0.031

OR, odds ratio; 95% CI, 95% confidence interval; AVVR, atrioventricular valve regurgitation; BNP, brain natriuretic peptide; CVP, central venous pressure; PA, pulmonary artery; SV-EDP, single ventricle-end diastolic pressure; SV-EDVI, single ventricle-end diastolic volume index; SV-EF, single ventricle-ejection fraction.

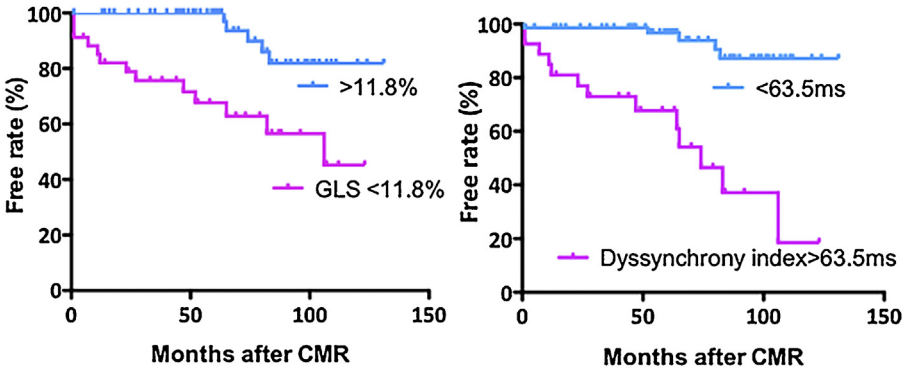

Fig. 2. Major adverse cardiovascular events (MACE)-free curves of two groups classified by global longitudinal strain (GLS) (left) and dyssynchrony index (right). Patients with GLS <11.8% (pink) had significantly lower MACE-free rates than those with coronal GLS ≥11.8% (blue). Patients with a dyssynchrony index ≥63.5 ms (pink) had significantly lower MACE-free rates than those with a dyssynchrony index <63.5 ms (blue). CMR, cardiac magnetic resonance.

GLS ≥11.8% ($n = 65$) had significantly higher MACE-free rates than those with GLS <11.8% ($n = 35$) (log-rank value = 14.15; $p = 0.0002$). Patients with a dyssynchrony index <63.5 ms ($n = 70$) had significantly higher MACE-free rates than those with a dyssynchrony index ≥63.5 ms ($n = 30$) (log-rank value = 28.17; $p < 0.0001$) (Fig. 2). A Cox hazard regression analysis showed that the hazard ratios were 6.825 (95% confidence interval, 2.51–18.56) for patients with GLS <11.8% and 21.69 (95% confidence interval, 6.96–67.56) for patients with a dyssynchrony index ≥63.5 ms for the development of MACE.

Discussion

The present study analyzed strain measurements obtained using CMR-FT to evaluate myocardial deformation and dyssynchronous contractions of patients after the Fontan procedure. This study demonstrated that patients with a small GLS or a larger dyssynchrony index were at higher risk for the development of MACE during the late phase of the Fontan procedure than those without. To the best of our knowledge, this is the first study to validate the predictive values of CMR-FT strain measurements for late phase mortality after the Fontan procedure. An increasing number of Fontan patients reach adulthood and present with sequelae of this palliative procedure [2,3,21,22]. Unfortunately, there are limited treatment options, such as heart transplantation and cardiac resynchronization therapy [23,24]. CMR-FT should be routinely analyzed as a promising technique to detect high risks for events and to determine follow-up management for adolescent Fontan patients.

Most progressive myocardial diseases predominantly cause subendocardial dysfunction during their early stages, leading to reductions in longitudinal left ventricular mechanics [14]. Using CMR-FT, GLS is probably the single most important variable that can be used to identify outcomes and for follow-up in Fontan patients because GLS is more reproducible and less variable than other parameters and has proven clinical value [19]. The present cohort consisted of Fontan patients covering the whole spectrum of single ventricular physiology, including morphologically dominant right or left ventricles and bi-ventricles. Cine imaging of the single ventricle showed more complex and various forms in the horizontal long-axis view or short-axis view than in the vertical long-axis view because the former included bi-ventricles (Fig. 3)

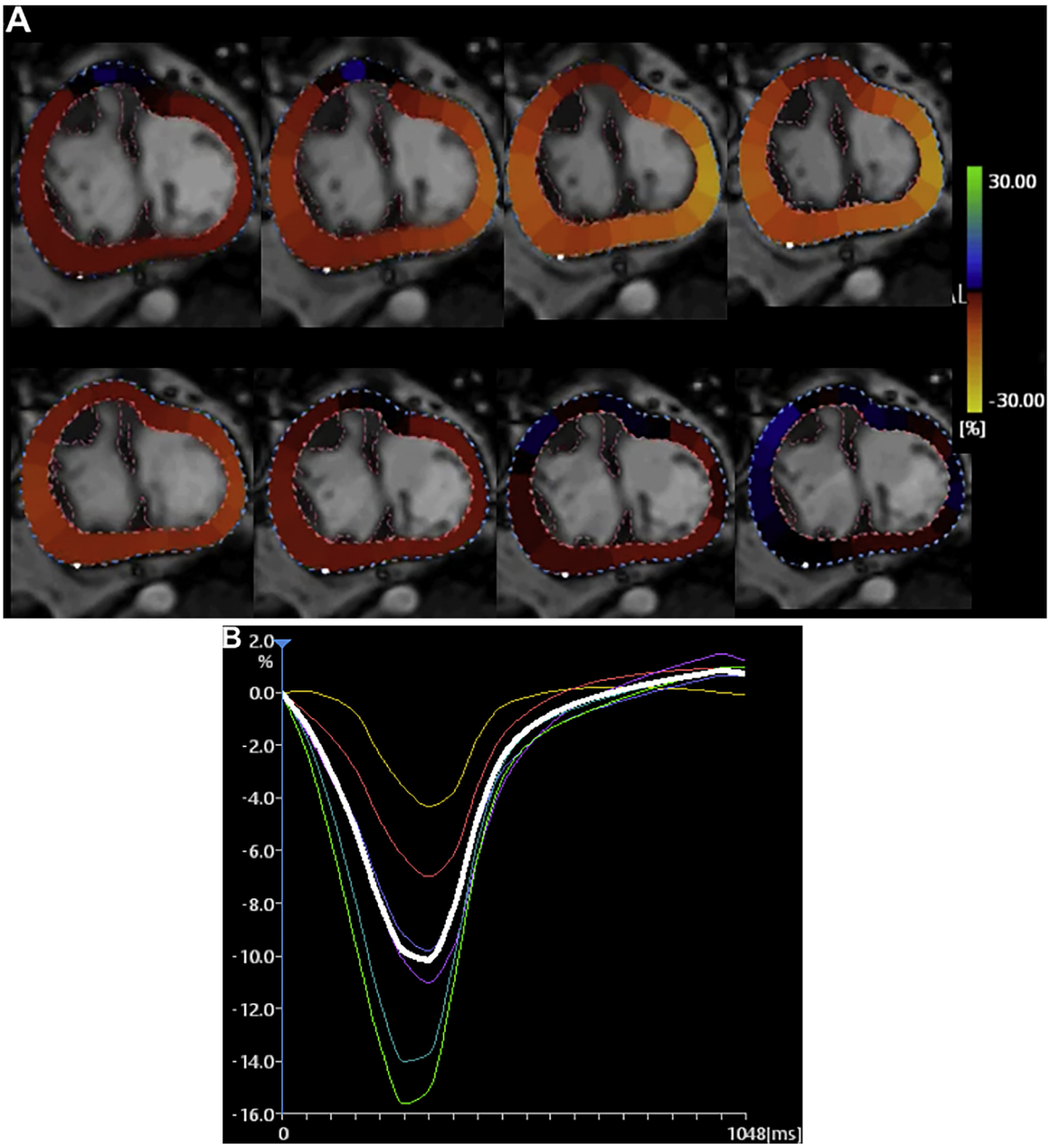

Fig. 3. A woman in her 30s who underwent the atrio-pulmonary connection Fontan operation to anatomically correct malpositioning of the great arteries, ventricular septum defect, and pulmonary stenosis 30 years previously. She developed protein-losing enteropathy and ventricular tachycardia 4 years later. (A) Feature-tracking analysis of short-axis cine imaging tracks the contours of the endocardium and epicardium in the systemic single ventricle throughout a cardiac cycle. The bi-ventricular type is similar to a cardioid. (B) Time curves of circumferential strain show the same peak time for six segments. The peak of the global strain (white line) was 10% and decreased.

and the latter scans only included the dominant ventricle with an aortic origin. Therefore, the vertical long-axis view is the best image for standardizing the wide spectrum of the single ventricle and for obtaining high reproducibility in strain measurements. The optimal cut-off of GLS for predicting MACE was 11.8%, which was almost equal to the GLS for patients with dilated cardiomyopathy and poor outcomes [19]. The GLS for non-MACE patients (mean, 13.8%) was lower than normal values for healthy adolescents (mean, 18%) and healthy adults (mean, 21%) reported in previous studies [25,26]. These results suggest that the single ventricle during the late phase of the Fontan operation, even if cardiac events have not occurred, has the potential for systolic impairment in comparison to the normal structural heart.

Interestingly, our proposed dyssynchrony index is able to predict MACE values for other parameters (Fig. 4). In contrast, the QRS width on electrocardiography was not associated with MACE. For the patients with functional single ventricles after Fontan procedure, the abnormal orientation of myofibers [27], myocardial fibrosis [28], and the absence of ventricular–ventricular interactions [29] may induce the development of dyssynchronous myocardial contractions. The morphology of ventricle and uniformity of ventricular wall might be concerned with the dyssynchrony index. The dyssynchrony index demonstrates variations in the contraction timing of six myocardial segments of the vertical long-axis single ventricle, thus reflecting the contraction delay between the basal and apical segments of systemic ventricle. Prolongation of systemic ventricular dyssynchrony might be associated with lower systolic pressure, lower cardiac output [20], and higher systemic venous pressure with failing Fontan circulation. Lower cardiac output could be because

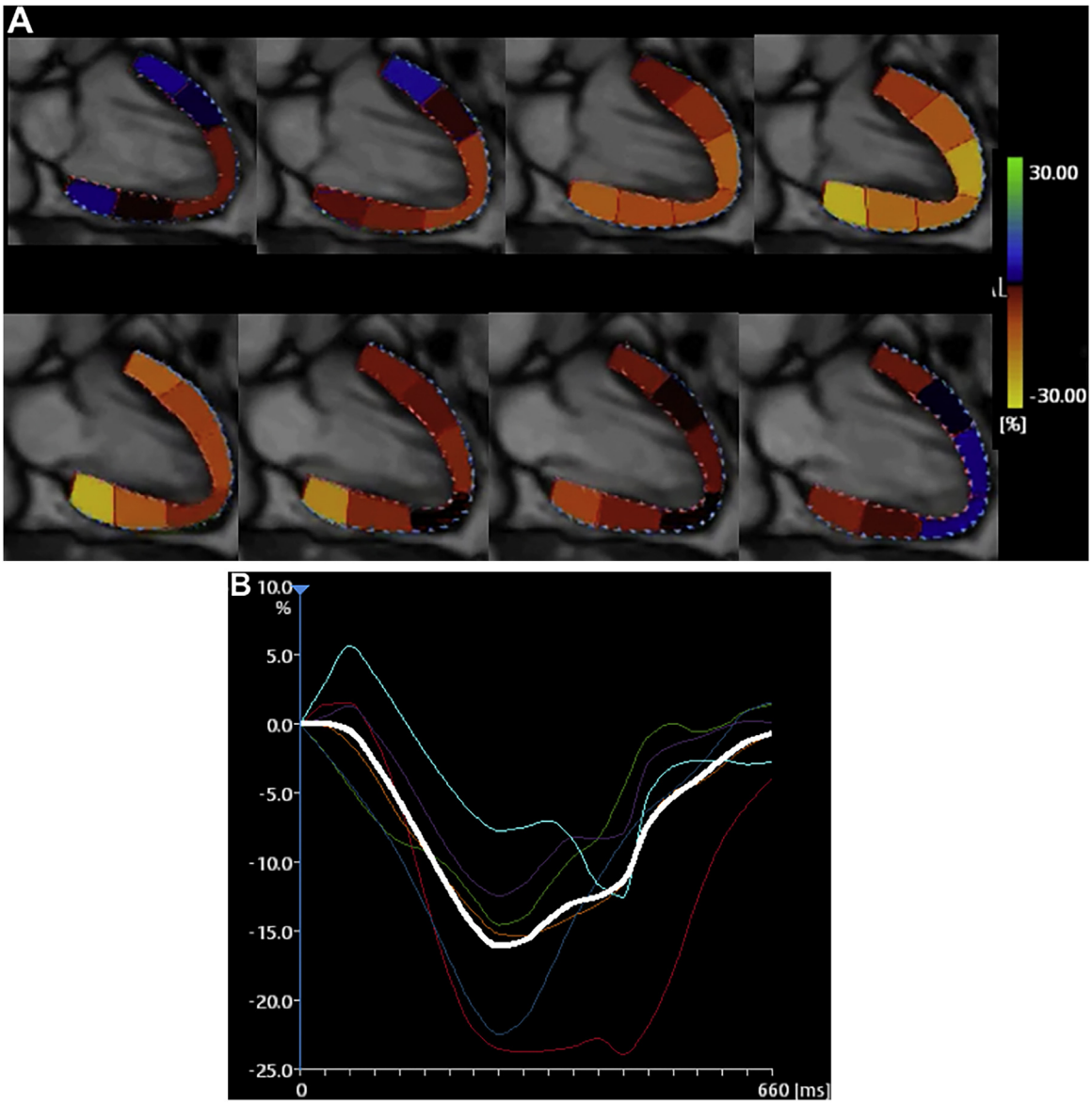

Fig. 4. A woman in her 30s (same as Fig. 3). (A) Feature-tracking analysis of vertical long-axis cine imaging shows separate hot color areas in the apical and basal segments at end-systole. (B) Time curves of longitudinal strain show the scatter peak times for six segments. Her global longitudinal strain (white line) was 15.5%. Her dyssynchrony index was 78 ms and prolonged.

of impaired intrinsic systolic ventricular function or underfilling of the systemic ventricle as a result of restricted transpulmonary blood flow. These phenomena are caused by dyssynchronous contraction of systemic ventricle, which leads to the development of MACE. Out of 18 patients with MACE, four patients underwent CRT due to refractory heart failure. One of the four patients died shortly after and the other three patients were alive without unscheduled hospitalization during the follow-up period. The former and latter were considered as CRT non-responder and responder. The dyssynchrony index and QRS width for a non-responder were 69 ms and 106 ms. The mean dyssynchrony index and QRS width for three responders were 104 ms and 118 ms. The dyssynchrony index was greater for CRT responder than non-responder, whereas there was no difference in QRS width between the two groups. The greater dyssynchrony index before CRT may be associated with good response after CRT. In adult CHD, interventricular dyssynchrony by CMR strain analysis was not related to QRS width. Wider QRS does not correspond to the presence of mechanical dyssynchrony [30]. In the present study, no correlation between QRS duration and the dyssynchrony index was observed (Pearson $r = 0.02$, $p = 0.89$). The presence of dyssynchrony depicted by CMR strain analysis is different from a delay on conducting system. Our proposed dyssynchrony index reflects mechanical dyssynchrony in systemic ventricle, and may be a more predictive marker in CRT response than QRS width.

Recently, Ohuchi et al. compared risk factors for adverse events in pediatric and adult Fontan cohorts and showed no associations between adverse events and dominant ventricle type or the presence of heterotaxy in adults [21]. These findings completely agreed with our results. Furthermore, there were no differences in the GLS and dyssynchrony index among the dominant ventricle types. We think that adolescent Fontan patients, who comprise a highly selective group after the loss of pediatric Fontan patients, likely represent a distinct phenotype. The existing understanding of cardiocentric modes of pediatric Fontan failure do not apply to the adult population.

Limitations

This study has multiple limitations. The generalizability of the findings may have been limited by retrospective analysis in its single-center design. Further, histologic and CMR studies have revealed regional variations in myocardial fibrosis in patients with functional single ventricles [28]. Therefore, the yield of myocardial deformation compared with CMR tissue characterization needs to be assessed. However, myocardial fibrosis using late gadolinium enhancement or T1 measurements was not analyzed in this study. In addition, the standard frame rate used for CMR (usually approximately 20–30 frames/cardiac cycle) was less than the recommended frame rates for speckle tracking echocardiography, which may have induced significant differences, especially when considering the strain rate values [27]. Although assessments of ventricular dyssynchrony using cine-tagging CMR with the standard frame rate have been reported for adult CHD [30], measuring diastolic function using the CMR-FT-derived strain rate has not been examined. The clinical utility of the strain rate should be investigated in future studies. The major advantages of CMR-FT are that it does not require special sequences and can be applied retrospectively. Therefore, this technique should be widely used as a helpful tool for the management of adolescent patients after the Fontan operation.

Conclusion

GLS and the dyssynchrony index of the single ventricle derived using CMR-FT are independent predictors of MACE during the late phase after the Fontan procedure and provide incremental information for risk stratification beyond clinical parameters, biomarkers, and standard CMR measurements.

Conflicts of interest

None.

Acknowledgments

This work was supported by the Japan Society for the Promotion of Science (JSPS) KAKENHI (16K10321). We thank Mr Yuichiro Sano and Mrs Seiko Shimizu of Canon Medical Systems Co. for technical assistance.

References

[1] Fontan F, Baudet E. Surgical repair of tricuspid atresia. Thorax 1971;26:240–8.
[2] Idorn L, Olsen M, Jensen AS, Juul K, Reimers JI, Sorensen K, et al. Univentricular hearts in Denmark 1977 to 2009: incidence and survival. Int J Cardiol 2013;167:1311–6.
[3] Allen KY, Downing TE, Glatz AC, Rogers LS, Ravishankar C, Rychik J, et al. Effect of Fontan-associated morbidities on survival with intact Fontan circulation. Am J Cardiol 2017;119:1866–71.
[4] Diller GP, Kempny A, Alonso-Gonzalez R, Swan L, Uebing A, Li W, et al. Survival prospects and circumstances of death in contemporary adult congenital heart disease patients under follow-up at a large tertiary centre. Circulation 2015;132:2118–25.
[5] Piran S, Veldtman G, Siu S, Webb GD, Liu PP. Heart failure and ventricular dysfunction in patients with single or systemic right ventricles. Circulation 2002;105:1189–94.
[6] Ohuchi H, Yasuda K, Miyazaki A, Iwasa T, Sakaguchi H, Shin O, et al. Comparison of prognostic variables in children and adults with Fontan circulation. Int J Cardiol 2014;173(277).
[7] Mori M, Hebson C, Shioda K, Elder RW, Kogon BE, Rodriguez FH, et al. Catheter-measured hemodynamics of adult Fontan circulation: associations with adverse event and end-organ dysfunction. Congenit Heart Dis 2016;11:589–97.
[8] Nakamura Y, Yagihara T, Kagisaki K, Hagino I, Kobayashi J. Ventricular performance in long-term survivors after Fontan operation. Ann Thorac Surg 2011;91(172).
[9] Kempny A, Diller GP, Orwat S, Kaleschke G, Kerckhoff G, ACh Bunck, et al. Right ventricular–left ventricular interaction in adults with tetralogy of Fallot: a combined cardiac magnetic resonance and echocardiographic speckle tracking study. Int J Cardiol 2012;154:259–64.
[10] Elder RW, Mccabe NM, Veledar E, Kogon BE, Jokhadar M, Rodriguez FH, et al. Risk factors for major adverse events late after Fontan palliation. Congenit Heart Dis 2015;10:159–68.
[11] Petko C, Hansen JH, Scheewe J, Rickers C, Kramer HH. Comparison of longitudinal myocardial deformation and dyssynchrony in children with left and right ventricular morphology after the Fontan operation using two-dimensional speckle tracking. Congenit Heart Dis 2012;7:16–23.
[12] Singh GK, Cupps B, Pasque M, Woodard PK. Accuracy and reproducibility of strain by speckle tracking in pediatric subjects with normal heart and single ventricular physiology: a two-dimensional speckle-tracking echocardiography and magnetic resonance imaging correlative study. J Am Soc Echocardiogr 2010;23:1143–52.
[13] Schmidt R, Orwat S, Kempny A, Schuler P, Radke R, Kahr PC, et al. Value of speckle-tracking echocardiography and MRI-based feature tracking analysis in adult patients after Fontan-type palliation. Congenit Heart Dis 2014;9:397–406.
[14] Obokata M, Nagata Y, VC-C Wu, Kado Y, Kurabayashi M, Otsuji Y, et al. Direct comparison of cardiac magnetic resonance feature tracking and 2D/3D echocardiography speckle tracking for evaluation of global left ventricular strain. Eur Heart J Cardiovasc Imaging 2016;17:525–32.
[15] Schuster A, Hor KN, Kowallick JT, Beerbaum P, Kutty S. Cardiovascular magnetic resonance myocardial feature tracking concepts and clinical applications. Circ Cardiovasc Imaging 2016;9:e004077.
[16] Truong UT, Li X, Broberg CS, Houle H, Schaal M, Ashraf M, et al. Significance of mechanical alterations in single ventricle patients on twisting and circumferential strain as determined by analysis of strain from gradient cine magnetic resonance imaging sequences. Am J Cardiol 2010;105:1465–9.
[17] Van Praagh S, Santini F, Sanders SP. Cardiac malposition with special emphasis on visceral heterotaxy (asplenia and polysplenia syndrome). Nadas' Pediatric Cardiology. Philadelphia: Hanley & Belfus; 1992. p. 589–608.
[18] Claus P, Salem AM, Pedrizzetti G, Sengupta PP, Nagel E. Tissue tracking technology for assessing cardiac mechanics principles, normal values, and clinical applications. JACC Cardiovasc Imaging 2015;8:1444–60.
[19] Buss SJ, Breuninger K, Lehrke S, Voss A, Galuschky C, Lossnitzer D, et al. Assessment of myocardial deformation with cardiac magnetic resonance strain imaging improves risk stratification in patients with dilated cardiomyopathy. Eur Heart J Cardiovasc Imaging 2015;16:307–15.
[20] Nagao M, Yamasaki Y, Yonezawa M, Kamitani T, Kawanami S, Mukai Y, et al. Geometrical characteristics of left ventricular dyssynchrony in advanced heart failure: myocardial strain analysis by tagged MRI. Int Heart J 2014;55:512–8.
[21] Ohuchi H, Kagisaki K, Miyazaki A, Kitano M, Yazaki S, Sakaguchi H, et al. Impact of the evolution of the Fontan operation on early and late mortality: a single-center experience of 405 patients over 3 decades. Ann Thorac Surg 2011;92:1457–67.
[22] Sugimoto M, Oka H, Kajihama A, Nakau K, Kuwata S, Kurishima C, et al. Non-invasive assessment of liver fibrosis by magnetic resonance elastography in patients with congenital heart disease undergoing the Fontan procedure and intracardiac repair. J Cardiol 2016;68:202–8.
[23] Ghelani SJ, Harrild DM, Gauvreau K, Geva T, Rathod RH. Comparison between echocardiography and cardiac magnetic resonance imaging in predicting transplant free survival after the Fontan operation. Am J Cardiol 2015;116:1132–8.
[24] Ohuchi H. Adult patients with Fontan circulation: what we know and how to manage adults with Fontan circulation? J Cardiol 2016;68:181–9.
[25] Taylor RJ, Moody WE, Umar F, Edwards NC, Taylor TJ, Stegemann B, et al. Myocardial strain measurement with feature-tracking cardiovascular magnetic resonance: normal values. Eur Heart J Cardiovasc Imaging 2015;16:871–81.
[26] Andre F, Robbers-Visser D, Helling-Bakki A, Foll A, Voss A, Katus HA, et al. Quantification of myocardial deformation in children by cardiovascular magnetic resonance feature tracking: determination of reference values for left ventricular strain and strain rate. J Cardiovasc Magn Reson 2017;19:8.
[27] Tham EB, Smallhorn JF, Kaneko S, Valiani S, Myeres KA, Colen TM, et al. Insights into the evolution of myocardial dysfunction in the functionally single right ventricle between staged palliations using speckle-tracking echocardiography. J Am Soc Echocardiogr 2014;27:314–22.
[28] Kato A, Riesenkamoff E, Yim D, Yoo SJ, Seed M, Grosse-Wortmann L. Pediatric Fontan patients are at risk for myocardial fibrotic remodeling and dysfunction. Int J Cardiol 2017;240:172–7.
[29] Fogel MA, Weinberg PM, Gupta KB, Rychik J, Hubbard A, Hoffman EA, et al. Mechanics of the single left ventricle a study in ventricular-ventricular interaction II. Circulation 1998;98:330–8.
[30] Nagao M, Yamasaki Y, Yonezawa M, Matsuo Y, Kamitani T, Yamamura K, et al. Interventricular dyssynchrony using tagging magnetic resonance imaging predicts right ventricular dysfunction in adult congenital heart disease. Congenit Heart Dis 2015;10:271–80.